Engineering and Technology Journal
Journal homepage: https://etj.uotechnology.edu.iq

Synthesis and characterization of nickel doped ternary oxide thin film as electrode materials for supercapacitor application

Cissan A. Sylvanus[a]*, **Jemima N. Ogwo**[a], **Sylvanus O. Isaac**[b]

[a] Physics Dept., Abia State University, PMB 2000, Abia State, Nigeria.
[b] Mechanical Engineering Dept., Abia State University, PMB 2000, Abia State, Nigeria.
*Corresponding author Email: cissan.sylvanus@abiastateuniversity.edu.ng

HIGHLIGHTS

- The measured refractive indexes of the Ni and Ag-doped thin films were negative.
- Lower scan rates enhance the electrochemical properties of the Ni-doped thin film.
- There is a reduction in agglomeration of the grains owing to the presence of Ni^{2+}.

ARTICLE INFO

Handling editor: Akram R. Jabur

Keywords:
Reduced graphene oxide (rGO)
ZnO
Ni dopant
Electrode material
Supercapacitor applications

ABSTRACT

The over-dependence on fossil fuels for energy generation, especially in developing countries like Nigeria, is a major setback to the economy. There is a hike in its price, hence the need to commercialize a renewable form of energy such as solar energy. Solar energy's intermittent nature is a barrier, requiring an efficient, affordable, clean energy storage mechanism such as a supercapacitor. Electrodes are a supercapacitor's basic components, and optimizing an electrode material leads to wide electrochemical applications. In this study, Ni-doped $CaAl_2O_3 - ZnO/rGO$ thin films were synthesized by electrochemical deposition, and the optical, morphological, and electrochemical properties were investigated through different characterization techniques. The optical properties were analyzed using a UV-Vis spectrophotometer, a decrease in absorbance (25%), absorption coefficient ($< 0.005 M^{-1}cm^{-1}$), extinction coefficient ($< 0.2\ M^{-1}m^{-1}$), real dielectric constant (< 2) and energy band gap (1.8 eV) of the film with the highest concentration of Ni was observed. The SEM result shows the films densely adhered to the substrate but unevenly distributed with imperfections (cracks and voids) as the concentration of Ni increases. The specific capacitance of the film ($Ni_{X=0.06}$) was measured to be 410.8 F/g, 235.7 F/g, and 184.2 F/g in the presence of 6M KOH electrolyte at a scan rate of 10 mV/s, 20 mV/s, 50 mV/s, respectively at the same current density of 0.3 A/g with the highest electrical conductivity of $9.41 \times 10^4\ ohm^{-1}m^{-1}$.These results indicate the promising features of Ni-doped $CaAl_2O_3 - ZnO/rGO$ thin films are used as electrode material for supercapacitor applications.

1. Introduction

The growing world population and technological advancements, such as the Internet of Things (IoT), 5G networks, etc., have increased the global demand for sustainable energy applications ranging from small-scale domestic to large-scale industrial applications.

Energy is vital for a nation's sustainable development and economic growth, hence the need for more abundant, reliable, non-depletable, cheap, and renewable energy sources in developing countries like Nigeria [1]. Globally, the efficiency of electrical power systems and constant power supply is a great concern to both the energy sector and the consumers of energy even though there is a global census to increase the share of renewable energy-based generation in the overall energy mix, transition to more environmental-friendly transportation with electric vehicles, and the liberalization of the electricity markets to ensure stability and sustainability in power network [2]. Solar energy has been used domestically and industrially for various purposes, such as electrification, heating, cooling, cooking, and space technology. Still, the consumption of solar energy and other renewable energy is minimal compared to fossil fuel consumption, as shown in Figure 1, the global primary energy consumption diagram [3]. This is due to the intermittent nature of renewable energy sources, hence the need for an efficient, reliable, durable, economical, and environmentally friendly renewable energy storage device such as a supercapacitor.

http://doi.org/10.30684/etj.2024.150129.1769
Received 09 June 2024; Received in revised form 03 July 2024; Accepted 03 July 2024; Available online 06 August 2024
2412-0758/University of Technology-Iraq, Baghdad, Iraq

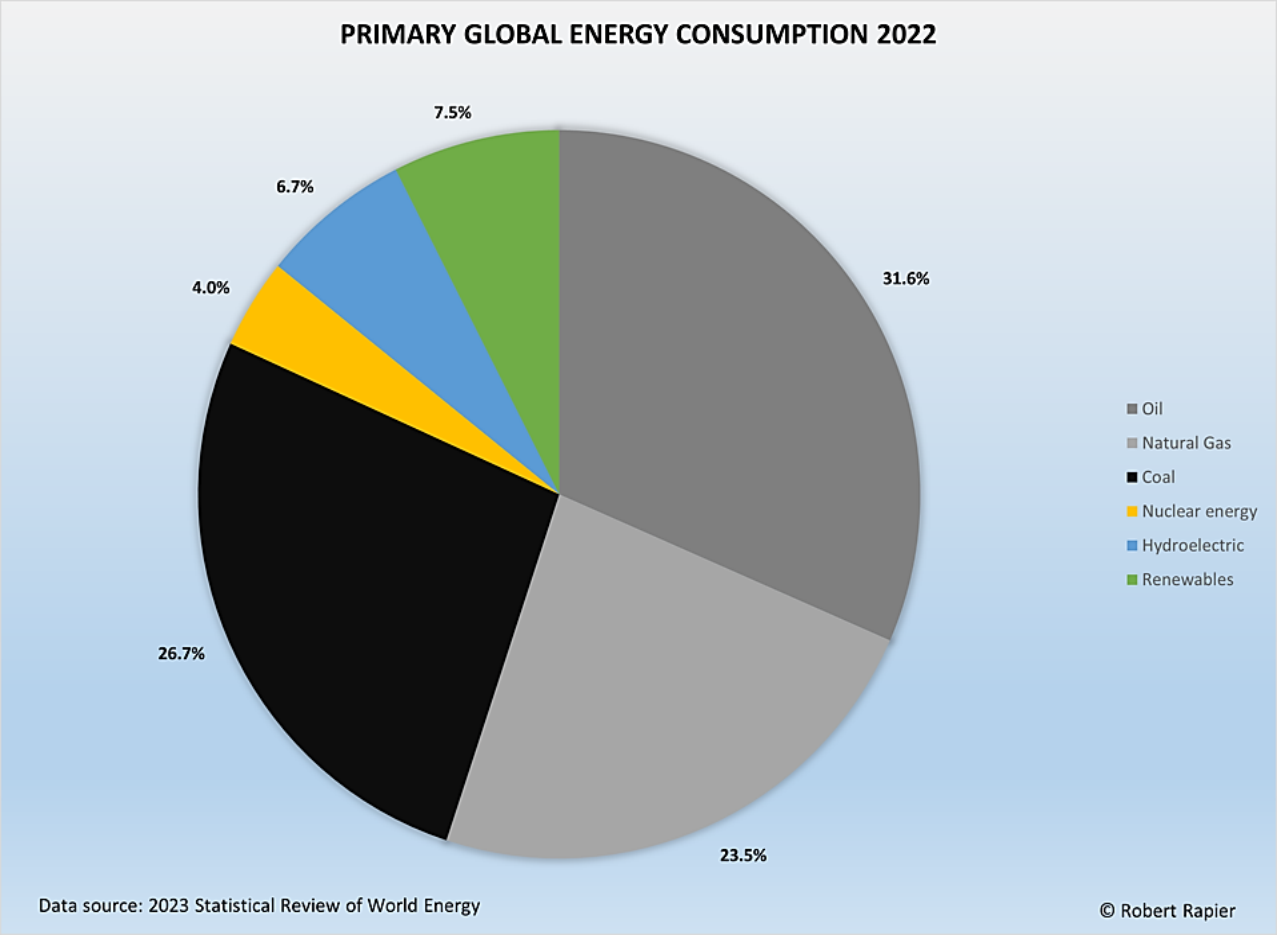

Figure 1: Statistical Review of Global Energy Consumption [3]

Electrodes are the main components of supercapacitors, and the ability to feasibly mass produce low-cost but high-energy density supercapacitor electrodes without compromising the micro/nanostructures of the material caused by restacking or aggregation is a hindrance to the deployment of supercapacitors into the national grid. Recently, many researchers have focused on hybridizing graphene with metal oxide nanoparticles to overcome irreversible agglomeration and other obstacles in obtaining stable reduced graphene oxide (rGO) sheets via the present reduction methods [4,5].

Several metal oxides (fe_2O_3, SnO_2, Co_3O_4, MnO_2, NiO, and WO_3) are supercapacitor electrodes for reversible redox reactions between electrolyte and electroactive materials. Still, most of them suffer from poor cycling performance, which means achieving overall high rate capability for high power performance is difficult due to their low electrical conductivity properties [5-7]. ZnO (semiconductors) based composite electrode materials can provide good electrochemical reversibility, high specific capacitance, high power density, high energy density, and good cycling stability, which make them promising materials for advanced supercapacitors [5-7]. Despite these desirable features of ZnO, it should be noted that the fabrication of p-type ZnO is rather difficult because of the low solubility of acceptor dopants, self-compensation effect, fast recombination of the electron-hole pairs, absorption of hydrogen impurities from the air which may act as a shallow donor, large band gap of 3.37 eV [6,8]. The control of these limitations led to the choice of the dopant and composite materials used in this study. Several studies on electrode materials highlighted the coupling mechanism between ZnO and rGO to facilitate better electronic transport; however, the synthesis of electrode material for supercapacitor application by electrochemical deposition technique is not commonly found in the literature. More so, studies regarding the relationship of $CaAl_2O_3$ and ZnO/rGO as electrode materials for application in energy storage devices does not exist in literature. This study aims to synthesize and characterize novel electrode material (Ni-doped $CaAl_2O_3 - ZnO/rGO$) suitable for energy storage devices (supercapacitors). Thus, a comprehensive study of Ni-doped $CaAl_2O_3 - ZnO/rGO$ was done to optimize synthesis parameters (i.e., dopant concentration, thickness, and reaction time) to obtain the desired composite thin films that can be used as electrode material in supercapacitors.

2. Materials and methods

2.1 Materials used

Table 1 shows the materials and analytical reagents used in this study. The reagents were used as received since they are of analytical grade.

Table 1: Materials and analytical reagents used in this study

S/N	Materials Used	Place of Purchase/ Manufacturer
1	Weighing Balance	FIN Lab Nigeria LTD
2	Beakers (different sizes)	FIN Lab Nigeria LTD
3	Spatula	FIN Lab Nigeria LTD
4	PH meter	FIN Lab Nigeria LTD
5	Detergent	FIN Lab Nigeria LTD
6	Magnetic Stirrer	FIN Lab Nigeria LTD
7	Deionized Water	FIN Lab Nigeria LTD
8	Microwave oven	FIN Lab Nigeria LTD
9	Fluorine-doped Tin Oxide FTO (substrate)	FIN Lab Nigeria LTD
	Reagents 1. Zinc sulphate heptahydrate ($ZnSO_4$ 2. Alumium Choride 6-hydrate ($AlCl_2$) 3. Sodium hydroxide (NaOH) 4. Nickel (ii) acetate 4-hydrate (NaOH) 5. Reduced graphene oxide (rGO) 6. Calcium sulphate ($CaSO_4$) 7. Potassium hydroxide (KOH) as electrolyte	MERCK (SIGMA –ALDRICH)

2.2 Synthesis of $CaAl_2O_3 - ZnO/rGO$

An already green synthesized graphene oxide (GO) was reduced following the procedures of another study [9]. The nanocomposite of GO was first mashed in a mortar before being thermally reduced at 400 °C for 4 hrs to reduce the GO into rGO. 0.2043g of thermally reduced graphene oxide (rGO) (x = 0.001 M) was dispersed in 20 ml of distilled water and stirred for 10mins yielding a stable rGO suspension which turned black without any observed precipitation. 2.875g of Zinc sulphate heptahydrate ($ZnSO_4$).$6H_20$ was mixed in 30 ml of de-ionized (DI) water and stirred for 45 min before adding to the rGO suspension. Also, 3.42 g of Aluminum chloride (VI) hydrate and 1.3614 g of calcium sulphate were dispersed separately in 10 ml of sodium hydroxide (0.1 M NaOH) to produce Al_2O_3 and CaO. Then, 10 ml of as-produced CaO and Al_2O_3 the suspension was added to ZnO/rGO. Then 1.3613 g of Nickel (ii) acetate tetrahydrate ($C_4H_{14}NiO_8$) was dispersed separately in 10 ml of sodium hydroxide (0.1 M NaOH) to produce the NiO dopant.

The electrochemical experiment was conducted in an electrochemical workstation (Autolab PGSTAT 204) under ambient conditions. The setup for the synthesis of these composite thin films was a conventional three-electrode configuration; the FTO, Ag/AgCl, and Carbon rod were the working, reference, and counter electrodes, respectively. The three electrodes were connected to a potentiostat at a deposition voltage of 5V for 60 s, and the deposition electrolyte consisted of 0.6 M KOH solution. FTO and stainless steel substrate were then immersed at different times in the prepared composite solutions for the absorption of the single-layer $CaAl_2O_3 - ZnO/rGO$ (control sample named CZ1). 5 ml of NiO made of different molar concentrations (x = 0.02, 0.04, 0.06 M) was added to the controlled sample, forming three different thin films labeled CZ 2, CZ 3, and CZ 4.

2.3 Characterization of thin film

The prepared samples were subjected to different characterization techniques such as optical analysis using UV spectrometer UV 3600 plus model, surface morphology using SEM, chemical composition using EDX, structural analysis using XRD, and electrochemical properties using CV, GCD, EIS, etc.

2.3.1 Optical characterization

The wavelength and absorbance of the films were read from the UV-Vis spectrometer. Transmittance refers to the amount of light that completely passes the sample and strikes the detector. The transmittance T for each deposited sample was deduced from the absorbance data for the same sample using the following relation given in Equation 1 [10].

$$T = 10^{-A} \tag{1}$$

where T = Transmittance and A = Absorbance.

The refractive index measures the bending of a light ray when passing from one medium to another. According to the research of Nwofe &Agbo [11], it has been established that optical reflectance is related to the refractive index n as seen in Equation 2:

$$n = \frac{1+\sqrt{R}}{1-\sqrt{R}} \tag{2}$$

where n = refractive index and R = optical reflectance.

Reflectance is the ratio of collected reflected radiant power to incident radiant power. Its value ranges from 0 to 1 due to laws of energy conservation.

$$R = 1 - (A + T) \quad (3)$$

where R =Reflectance, A =Absorbance and T = Transmittance

The absorption coefficient is a measure of the rate of decrease in the intensity of electromagnetic radiation as light passes through a given substance. It was evaluated from the optical absorbance data using the relation in Equation 4 [12].

$$\alpha = {2.302A}/{t} \quad (4)$$

where A = Absorbance and t = film thickness

The Extinction Coefficient k is described in Equation 5 as:

$$k = \frac{\alpha\lambda}{4\pi} \quad (5)$$

where α = optical absorption coefficient and λ= wavelength [13, 14].

The dielectric constant refers to the ratio of the material's electric permeability to free space's electric permeability. The complex dielectric constant $\varepsilon = \varepsilon_r + j\varepsilon_i$ is a foundational intrinsic property of the material. The real part (ε_r) of the dielectric constant is associated with the term that shows how much it will slow down the speed of light in the material and the imaginary part (ε_i) shows how a dielectric absorbs energy from an electric field due to dipole motion [15]. The dielectric constant (real and imaginary) can be evaluated from refractive index (n) and extinction coefficient (k) using the following relations in Equations 6 and 7 [16, 17]: For the real part;

$$\varepsilon_r = n^2 + k^2 \quad (6)$$

For imaginary part;

$$\varepsilon_i = 2nk \quad (7)$$

Energy band gap refers to the energy difference between the top of the valence band and the bottom of the conduction band. The energy gap (E_g) will be estimated by assuming a direct transition between valence and conduction bands from the expression in Equation 8 [18]

$$(\alpha hv)^r = A(hv - E_g) \quad (8)$$

where r=2 (direct allowed transitions), Equation 8 yields Equation 9

$$(\alpha hv)^2 = A(hv - E_g) \quad (9)$$

Optical conductivity (σ_0) is the optical response of a transparent solid [19]. Equation 10 gives the mathematical formula.

$$\sigma_0 = \frac{\alpha nc}{4\pi} \quad (10)$$

where c = speed of light, α = absorption coefficient and n = refractive index.

3. Results and discussion

3.1 Surface morphology and elemental composition

Figure 2a shows an agglomerated, densely packed, non-uniform grains of the undoped sample due to the presence of graphene. The presence of agglomeration could inhibit the diffusion of electrolyte ions inside the pores, thereby reducing the specific capacitance of the material [20]. Figures 2b-d show a reduction in grain agglomeration due to the presence of Ni^{2+}. The films densely adhered to the substrate, forming grain boundaries as the concentration of Ni increased, increasing grain sizes. This is contrary to the findings of another study [21] but agrees with other literatures [20, 22, and 23]; an increase in grain size promotes the capacitance of the film due to increased surface area, hence suitable for use as an electrode material for supercapacitor applications. At 4% Ni^{2+}doped thin film, uniform small granules exist, indicating its unique morphological features and suggesting the possibility of obtaining reduced graphene thin films with metal oxides and semiconductors suitable for.

The EDX result reveals the elements in the composite films, as seen in Figure 3a,b. It shows the abundance of different elements in the samples extracted from energy-dispersive X-ray spectroscopy (EDX). As observed, Oxygen (O) is the most abundant element in all composites with an atomic ratio of 40.5 compared to Zn, and the absence of hydrogen is due to the fact that it does not emit X-rays. The presence of 0.2 and 0.6 % Ni can be seen in the Figures 3a and 3b respectively, which mainly shows the lower boundary of a typical EDX system. The non appearance of Ca in the EDX results was observed and this could be attributed to the film thicknesa and the oxidation of the surface of calcium (Ca).

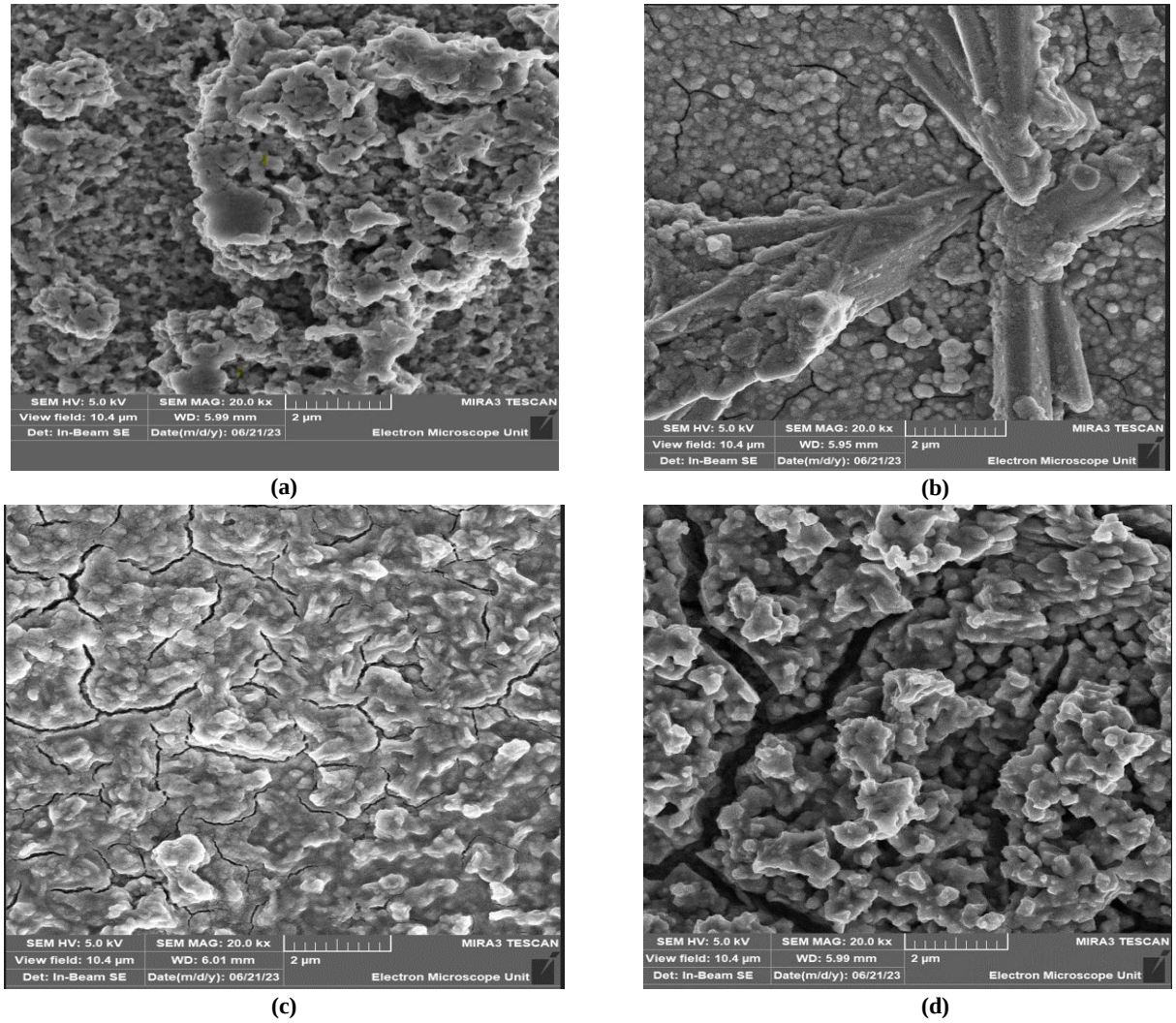

Figure 2: Morphological Analysis of Ni-doped $CaAl_2O_3 - ZnO/rGO$ films (a) CZ 1 b) CZ 2 (c) CZ 3 (d) CZ 4

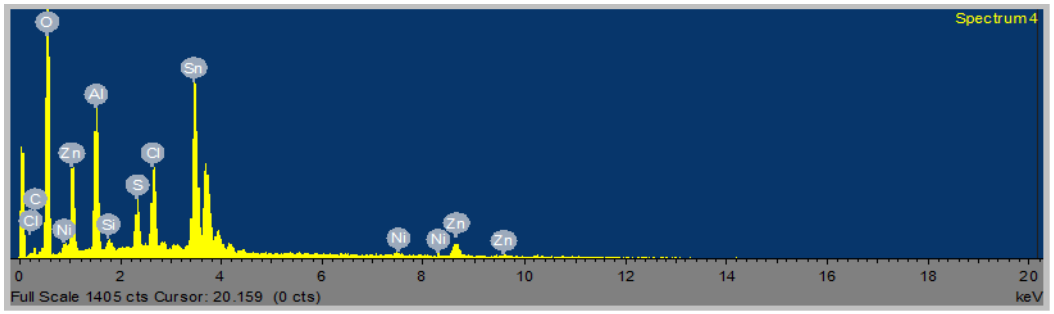

(a)

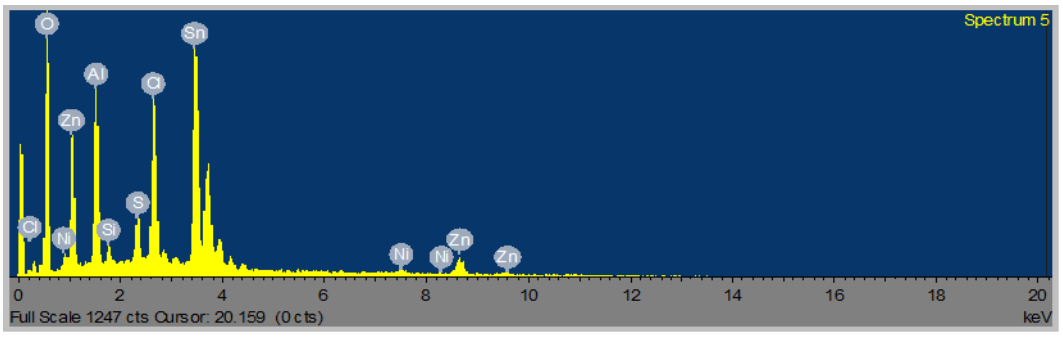

(b)

Figure 3: (a,b) Elemental composition of Ni-doped $CaAl_2O_3 - ZnO/rGO$ films by EDX Technique

3.2 Optical analysis

3.2.1 Transmittance and absorbance spectra

The absorbance A decreased at higher wavelengths for all samples, with a distinctive decrease for the sample with the highest concentration of Nickel between 850 nm and 1000 nm, as shown in Figure 4a. This result contradicts the findings in some literatures [22-24], where only the optical properties of Ni-doped ZnO were investigated. Therefore, this decrease in absorbance at the highest concentration of Ni within the UV region of the electromagnetic spectrum could be attributed to the plasmon effect of the C–C bond in graphitic structure and of the sp^2 bonding of C=C from benzene ring in rGO materials respectively [23] and the concentration quenching effect between the neighboring atoms of $Ni^{2+}$and Zn^{2+} [25]. The absorption peak of ZnO–rGO occurred at 380 nm [23], similar to the results obtained for all samples in this present study.

According to Figure 4b, 60% transmittance was recorded within the ultraviolet-visible region for the highest concentration of Nickel, but persistent transmittance within the wavelength range of 850 to 1000 nm was reported in another study of doped ZnO. This was attributed to increased surface roughness caused by the dopant, which reduces the dispersion of light and improves transmittance [26]. Unlike other samples, the undoped and $Ni_{x=0.04}$ doped thin films have smooth curves and presence of interference pattern, which indicates the films' homogeneity and thickness above 100 nm [27]. Spikes in the absorption edge from blue shift to red shift can be observed between 700 and 900 nm for the sample with the highest concentration of Ni dopant; it could be due to enhanced oxygen sites in ZnO thin films [20].

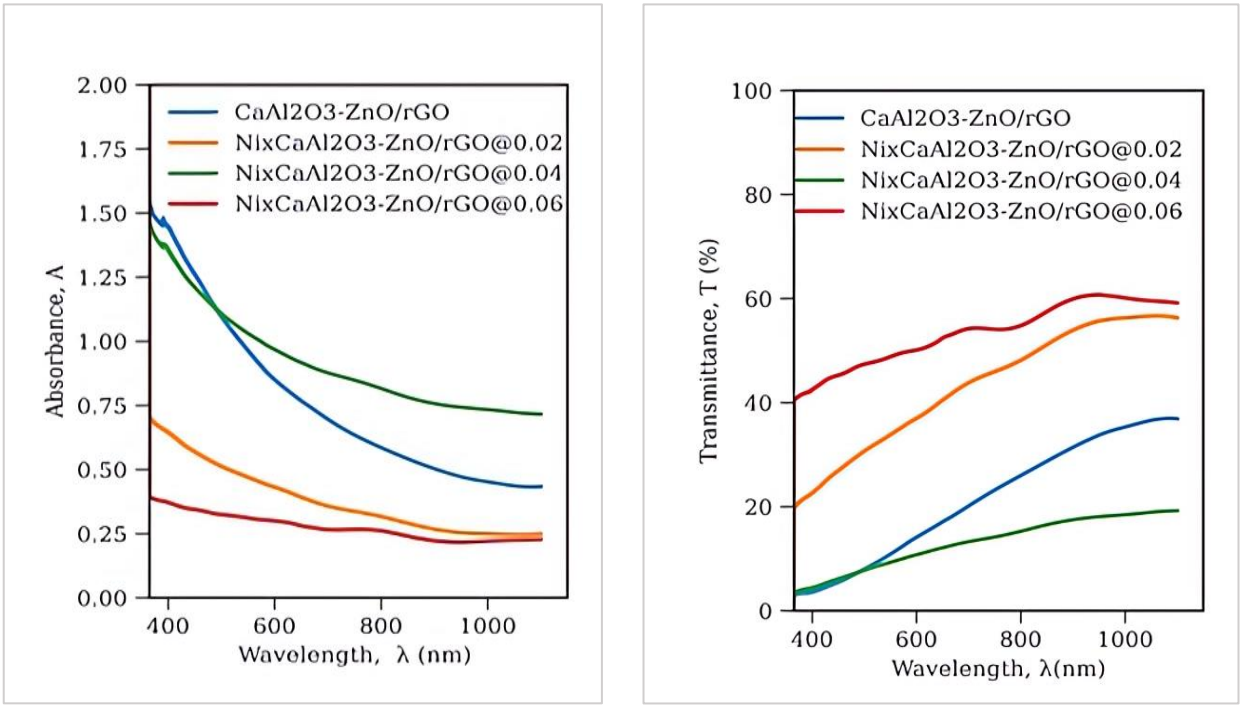

(a) **(b)**

Figure 4: a) Absorbance spectra b) Transmittance spectra for CZ 1, CZ 2, CZ 3, CZ 4

3.2.2 Refractive index and reflectance

The refractive index (n) is an important factor in fabricating devices with good optical properties because dispersion energy depends on the material's optical transition and optical conductivity [28]. Figure 5a shows that the measured refractive indexes of the Ni and Ag-doped thin films were negative and decreased for the undoped and $Ni_{x=0.04}$ doped thin films as the photon energy increased. This is attributed to the decrease in absorbance and the scattering of light [29]. The film is useful for supercapacitor applications due to its reduced refractive index.

The reflectance of Ni-doped thin films increased to 20% at 0.06M of Ni^{2+} and 15% at 0.02M of $Ni^{2+}$with a decrease for the 0.04M of Ni^{2+} between 300nm-400nm, as shown in Figure 5b. This is an indication of an increase in the number of isolated centers and substitution defects located in the $CaAl_2O_4 - ZnO/rGO$ host matrix, which was truncated at 0.04M of Ni^{2+} due to the structure of the matrix and the synthesis technique employed; this could cause an inhomogeneous distribution of cations with segregation within the layers of the same source [25]. This is contrary to another report [23].

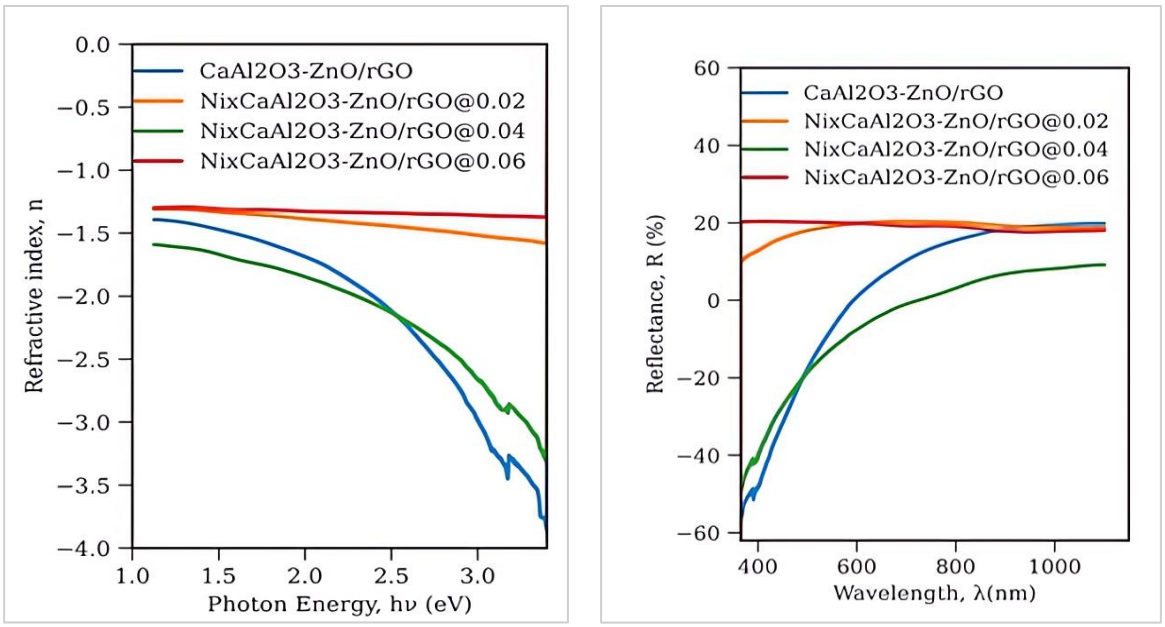

Figure 5: a) Refractive index, b) reflectance spectra for CZ 1, CZ 2, CZ 3, CZ 4

3.2.3 Absorption coefficient and extinction coefficient

The highest concentration of Ni (0.06M) has the lowest absorption and extinction coefficients as shown in Figures 6a and 6b. However, a slight increase in extinction coefficient can be observed within the wavelength range of 600-1000 nm, according to Figure 6a. A decrease in absorption coefficient occurred in all samples within the UV region. While the reverse is the case for the extinction coefficients, notably the increase in extinction coefficient along wavelength of 500-1000 nm for the 4% Ni-doped thin film. The intensity of the absorption coefficient decreases abruptly due to the presence of nickel ion (Ni^{2+})This means more oxygen ions would be attracted to $Ni^{2+}$to form NiO interstitial sites [22, 25]. A thicker emitter layer is necessary to reduce the effect of spectra overlap on the electrode's performance. This overlap could be due to the complexity of the thin film materials used in this study.

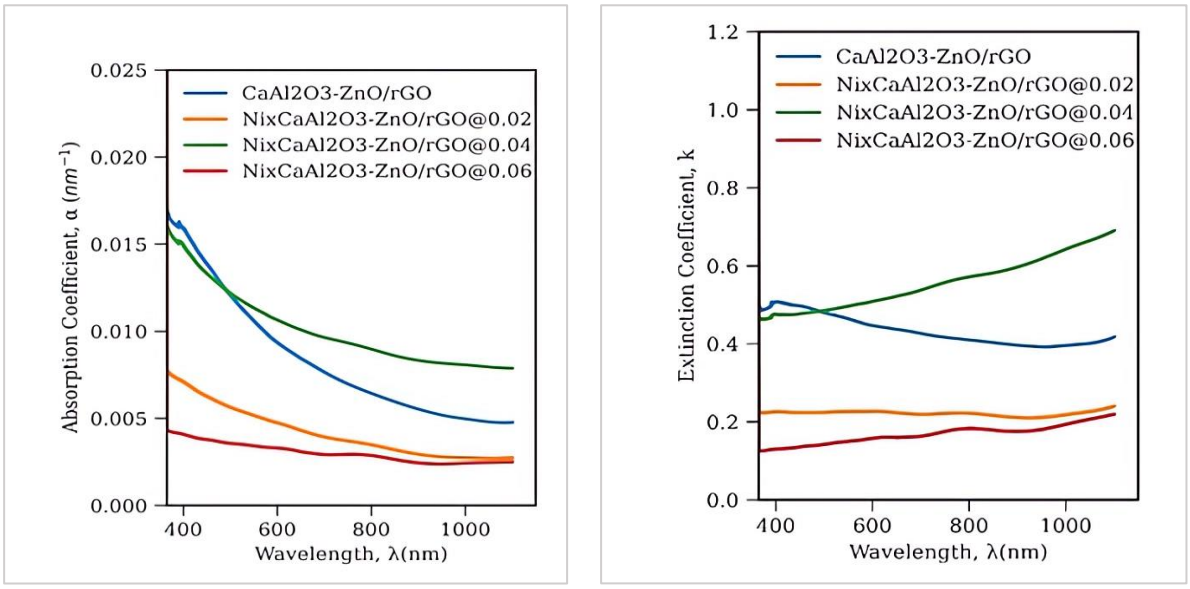

Figure 6: a) Absorption coefficient, b) Extinction coefficient for CZ 1, CZ 2, CZ 3, CZ 4

3.2.4 Dielectric constant

Figures 7a and b shows the spectra of the real and imaginary dielectric constant, the imaginary values of Ni-doped $CaAl_2O_3 - ZnO/rGO$ thin films increased mostly with the highest concentration of Ni, but a drop across higher wavelengths was observed in Figure 7a. This increase will promote the capacitance of the deposited material, thereby increasing the energy density. On the contrary, the real values of the dielectric constant decreased drastically in the presence of Ni dopant across higher wavelengths except for 0.04 M of Ni as seen in Figure 7b; a decrease in both the real and imaginary values of the

dielectric constant along higher wavelengths as the doping ratio increases was observed [30] This could be attributed to strong interaction between electrons and photons at this concentration of Ni and these low values reveal the composite thin film is a good material for tunable capacitor applications [31].

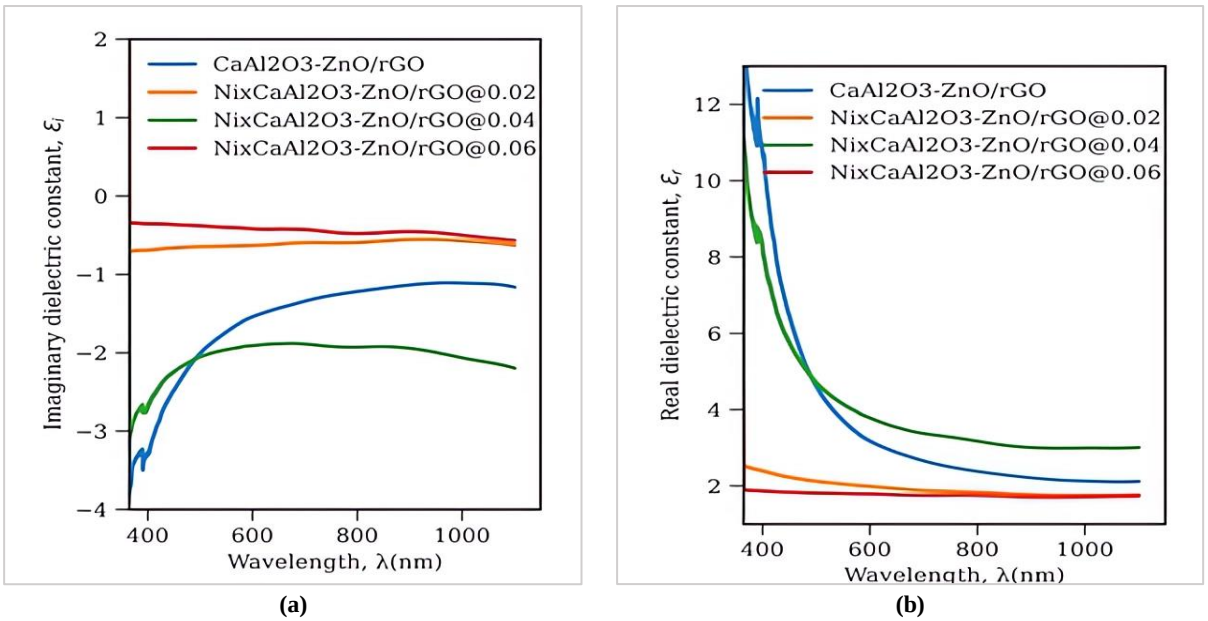

Figure 7: a) Imaginary dielectric constant, b) Real dielectric constants for CZ 1, CZ 2, CZ 3, CZ 4

3.2.5 Energy band gap (E_g)

For allowed direct transitions, where α = absorption coefficient, h = Planck's constant, v = frequency, Eg = energy band gap, and A = constant, which depends on the materials. Where A is a constant, the exponent r equals 2 and 1/2 for direct and indirect allowed transitions, respectively. Since ZnO is known to be a direct semiconductor, we have chosen the exponent r = 2 [32]. The energy band gap decreased from 2.2 eV for undoped $CaAl_2O_3 - ZnO/rGO$ thin films to 2.17 eV, 2.10 eV, and 1.8 eV for Ni-doped $CaAl_2O_3 - ZnO/rGO$ thin films, as shown in Figure 8, show there is an interaction of Ni^{2+}on entering the crystal lattice of $CaAl_2O_3 - ZnO/rGO$ [25]. This indicates improvement in the conductivity and crystalline nature of the material [33], making it a suitable electrode material.

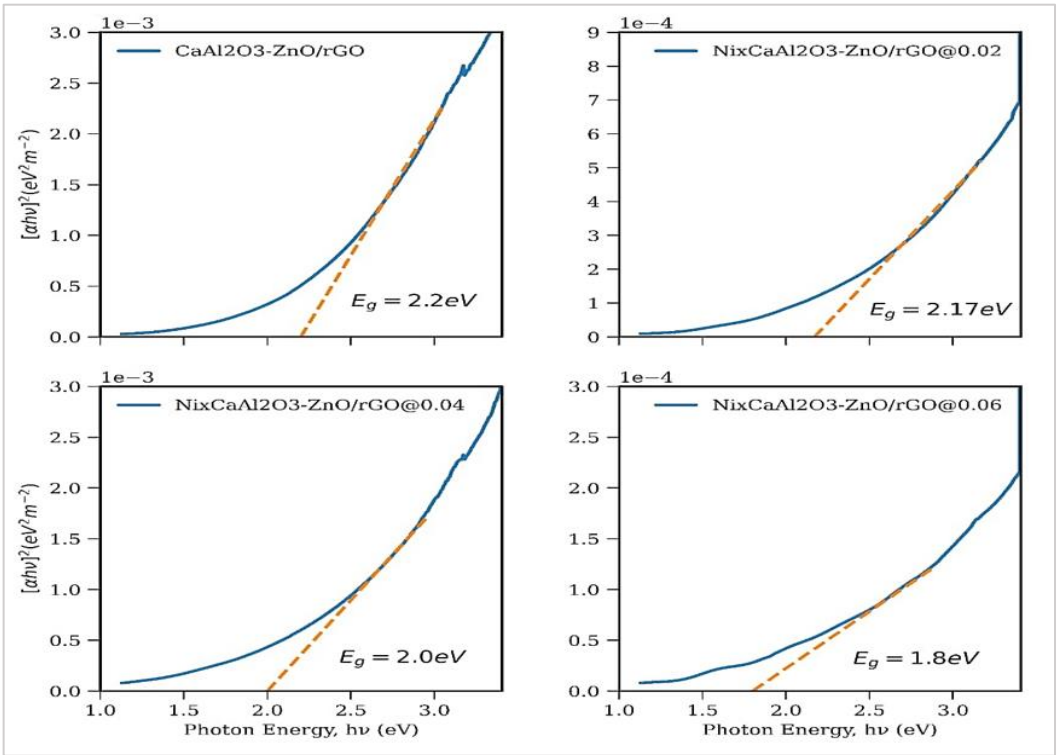

Figure 8: Tauc's plot of CZ 1, CZ 2, CZ 3, and CZ 4

3.2.6 Optical conductivity

The optical conductivity of Ni-doped $CaAl_2O_3 - ZnO/rGO$ thin films increased with an increase in Ni concentration and remained constant at higher photon energy values, as seen in Figure 9, though an intermediate drop exists. The implication is that the incorporation of Ni^+into the reaction medium influences the optical conductivity of the deposited thin film. An increase in the density of localized states in the energy band could cause an increase in the optical conductivity of the films [34]. Low absorption coefficient and refractive index values imply a decrease in optical conductivity. As Ni content rises to 6%. Optical conductivity rises with increasing Ni doping levels and is invariant along the energy band.

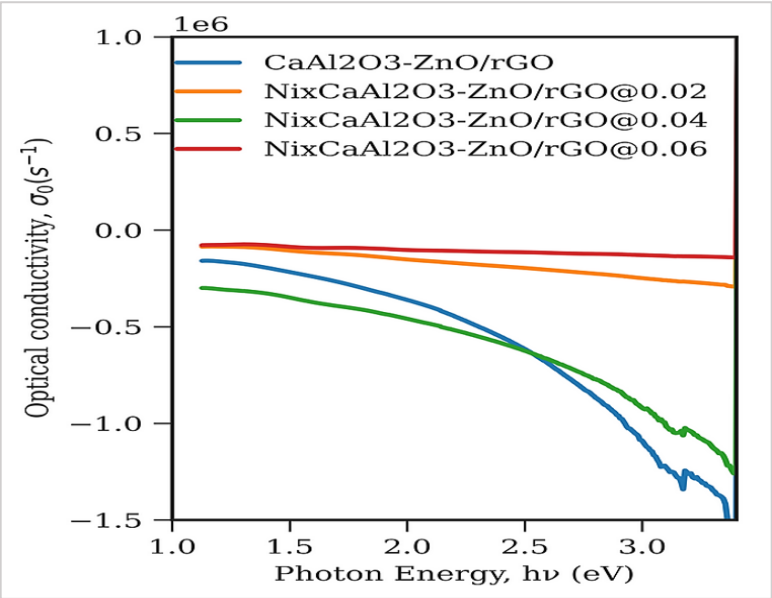

Figure 9: Optical conductivity versus Photon energy of CZ 1, CZ 2, CZ 3, CZ 4

3.3 Electrochemical analysis

The electrochemical properties of the Ni-doped $CaAl_2O_3 - ZnO/rGO$ thin films were analyzed using a three-electrode cell configuration with a 0.6 M KOH electrolyte within the potential range of -0.4 to 0.4 V at scan rates of 10 mV/s, 20 mV/s, 50 mV/s, the cyclic voltammograms (CV) of the electrode samples are shown in Figures 10. The films show rectangular shapes at low scan rates. The specific capacitance of the $Ni_{x=0.06}$ doped thin films (CZ 3) was evaluated using Equation 11 because it has the best shape without redox peaks compared to other samples.

$$C_{sp} = \frac{A}{2 \times m \times k\,(V_2 - V_1)} \tag{11}$$

Here, A is the integrated area of the curve, m is the mass of the film, k is the scan rate, and V is the potential window. The specific capacitance of Ni-doped (6%) thin films (CZ 3) at the same current density of 0.3 A/g are 410.8 F/g, 235.7 F/g, and 184.2 F/g at scan rates of 10 mV/s, 20 mV/s, 50 mV/s respectively.

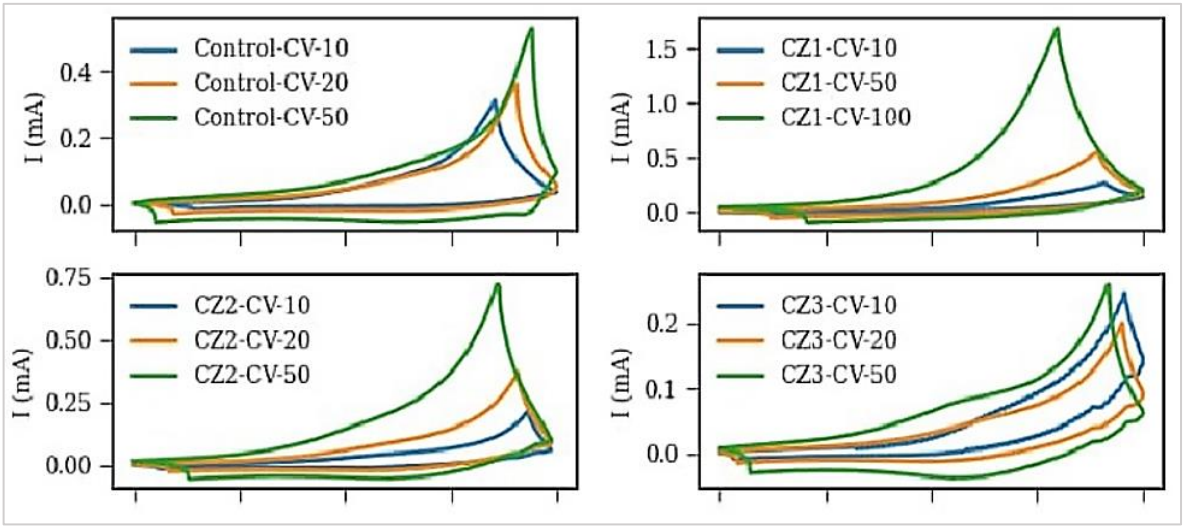

Figure 10: Cyclic voltammograms (CV) of Ni-doped $CaAl_2O_3 - ZnO/rGO$ thin film

The electrical properties of the undoped and Ni-doped thin films are seen in Table 2. It can be seen that the film with the highest concentration of Ni has the lhighest values of conductivity (9.41E+04 $\Omega^{-1}m^{-1}$). This shows the effect of concentration on the electrical properties of the doped films.

Table 2: Electrical Properties of Ni-doped $CaAl_2O_3 - ZnO/rGO$ thin film

Samples	Resistance (Ω)	Sheet Resistance (Ω)	Resistivity (Ωm)	Conductivity ($\Omega^{-1}m^{-1}$)
Undoped $CaAl_2O_3 - ZnO/rGO$	9.11E+00	4.12E+01	8.75E-06	1.14E+05
Ni@0.02M	-5.59E+00	-2.53E+01	-5.33E-06	-1.88E+05
Ni@0.04M	-2.09E+02	-9.46E+02	-1.98E-04	-5.05E+03
Ni@0.06 M	1.13E+01	5.09E+01	1.06E-05	9.41E+04

Considering Tables 3 and 4, the potential varied linearly at different speeds of 10, 20, and 50 per second (scan rates), the galvanostatic charge and discharge values, energy density, and power density of the undoped and doped films are presented. Improving the properties of the film can be seen when comparing the doped and undoped values. Lower scan rates favor the electrochemical properties of this Ni-doped film; at 10 mV/s, the $Ni_{x=0.06}$ doped $CaAl_2O_3 - ZnO/rGO$ thin film has the highest energy density of 131.46 Wh/Kg and power density of 15.7754386 KW/Kg.

Table 3: Electrochemical Properties of $CaAl_2O_3 - ZnO/rGO$ thin film obtained at different scan rates

Scan rate	Q_c ($mAhKg^{-1}$)	Q_d ($mAh\ g^{-1}$)	Energy density W h Kg^{-1}	Power density KW Kg^{-1}
10 mV/s	60.19417476	7.223300971	2166.990291	541.7476
20 mV/s	50.48543689	6.058252427	1817.475728	454.3689
50 mV/s	39.61165049	4.753398058	1426.019417	356.5049

Table 4: Electrochemical Properties of $Ni_{x=0.06}$ doped $CaAl_2O_3 - ZnO/rGO$ thin film (CZ3) obtained at different can rates

Scan rate	Q_c ($mAh\ Kg^{-1}$)	Q_d ($mAh\ g^{-1}$)	Energy density W hKg^{-1}	Power density KW Kg^{-1}
10 mV/s	4732.631579	1183.158	131.4619883	15.7754386
20 mV/s	2715.789474	678.9474	75.43859649	9.052631579
50 mV/s	2122.105263	530.5263	58.94736842	7.073684211

4. Conclusion

This study employed an electrochemical deposition technique to synthesize hexagonal Ca efficiently$Al_2O_3 - ZnO/rGO$ thin film doped with Ni as an electrode material for supercapacitor application. The films were then characterized using various methods such as UV-Vis, Cyclic Voltametry, GCD, EDX, and SEM. Results show that the peak of the transmittance spectra was 60 % at $\sim 900\ nm$ and optical energy band gap (Eg) of 1.8 eV for the film with the highest concentration of Ni dopant (0.06 M) w, suggesting its suitability for supercapacitor application. The surface morphology shows the films densely adhered to the substrate but unevenly distributed with grain boundaries. The higher concentration of Ni reduces agglomeration caused by the presence of graphene but enlarges the grain sizes. A specific capacitance of 410.8 F/g, 235.7 F/g and 184.2 F/g at a scan rate of 10 mV/s, 20 mV/s, 50 mV/s respectively were evaluated. The results presented imply Ni-doped $CaAl_2O_3 - ZnO/rGO$ thin film could be a new electrode material for supercapacitor application and may be optimized for the commercialization of supercapacitors into the national grid. A novel method of synthesis, increased dopant concentration, lower can rates, and different electrolytes could be used in the future to study Ni-doped $CaAl_2O_3 - ZnO/rGO$ thin film. Also, peak fitting residual spectrum analysis can be used in further studies for accurate elemental detection.

Author contributions

Conceptualization, C. Sylvanus and J. Ogwo; data curation, S. Isaac.; formal analysis, C. Sylvanus.; investigation, C. Sylvanus.; methodology, C. Sylvanus; project administration, J. Ogwo, resources, C. Sylvanus and S. Isaac.; software, C. Sylvanus.; supervision, J. Ogwo; validation, J. Ogwo., C. Sylvanus.; and S. Isaac.; visualization, S. Isaac.; writing—original draft preparation, C. Sylvanus; writing—review and editing, C. A. Sylvanus. All authors have read and agreed to the published version of the manuscript.

Funding

This research received funding Tertiary Education Trust Fund (TETFUND).

Data availability statement

The data that support the findings of this study are available on request from the corresponding author.

Conflicts of interest

The authors declare that there is no conflict of interest.

References

[1] C. A. Sylvanus, G. U. Chukwu, S. O. Isaac, Evaluation of Solar Constant for Sustainable Renewable Energy Generation in Ikwuano L. G. A, Abia State of Nigeria, Afr. J. Renewable Altern. Energy, 4 (2019) 109-120.

[2] C. A. Sylvanus, E. Nwaokoro, Comparison of Supercapacitors and Superconducting Magnets as Energy Stor-age Systems, Niger. J. Physics., 29 (2020) 138-145.

[3] Rapier, R. Global Energy Trends: Insights From The 2023 Statistical Review Of World Energy, Forbes Newsletter, 2022.

[4] Gao, W. Electrochemical and electromechanical stud-ies on nanostructured electrodes for super-capacitors. Ph.D. Thesis, submitted to Analytical chemistry Sorbonne Univer-sité, 2018.

[5] PauPing, W. C. Synthesis of reduced graphene ox-ide/tungsten trioxide nanocomposite electrode for high elec-trochemical performance. Dissertation submitted to the Insti-tute of Graduate Studies University of Malaya Kuala Lum-pur, 2017.

[6] M. Buldu-Akturk, M. Toufani, A. Tufani, E. Erdem, ZnO and reduced graphene oxide electrodes for all-in-one supercapacitor devices, Nanoscale , 14 (2022) 3269-3278. https://doi.org/10.1039/D2NR00018K

[7] R. T. Ngaloy, A. M. Fontanilla, M. S. Rebecca Soriano, C. S. Pascua, Y. Matsushita, L. A. Agulo, Highly efficient photocatalysis by zinc oxide-reduced graphene oxide (zno-rgo) composite synthesized via one-pot room-temperature chemical deposition method, J. Nanotechnol., 2019 (2019) 1-11 . https://doi.org/10.1155/2019/1895043

[8] R. Elshypany, H. Selim, K. Zakaria, A. H. Moustafa, S. A. Sadeek, S. I. Sharaa, P. Raynaud and A. A. Nada, Magnetic ZnO crystal nanoparticle growth on re-duced graphene oxide for enhanced photocatalytic perfor-mance under visible light irradiation, Molecules, 26 (2021) 2269. https://doi.org/10.3390/molecules26082269

[9] A. R. Ansari, S. A. Ansari, N. Parveen, M. O. Ansari and Z. Osman, Silver nanoparticles embedded on re-duced graphene oxide @ copper oxide nanocomposite for high performance supercapacitor applications, Materials 14 (2021) 5032. https://doi.org/10.3390/ma14175032

[10] E. C. Nwaokorongwu, N. I. Akpu, & U. I. Joseph, Growth and optical characterization copper sulphide thin films by sol-gel technique, Int. J. Innovative Sci. Eng. Technol. Res., 6 (2018) 38-44. http://dx.doi.org/10.13140/RG.2.2.25332.37768

[11] P.A. Nwofe, P.E. Agbo, Effect of deposition time on the optical properties of cadmium sulphide thin films, Int. J. Thin Films Sci. Technol., 4 (2015) 63-67. http://dx.doi.org/10.12785/ijtfst/040201

[12] M. Jayandran, M. M. Haneefa & V. Balasubramanian, Green synthesis and characterization of Manganese nanoparticles using natural plant extracts and its evaluation of antimicrobial activity., J. App Pharm Sci, 5 (2015) 105-110. http://dx.doi.org/10.7324/JAPS.2015.501218

[13] P.E. Agbo, P.A. Nwofe, C.A. Elekwa, M.N. Nnabuchi, Comparative Study of the Optical Properties of CdZnS Deposited by Two methods, J. Ovonic Res., 12 (2016) 163–169.

[14] M. H. Suhail & R. A. Ahmed, Structural, optical and electrical properties of doped copper ZnS thin films prepared by chemical spray pyrolysis technique, Adv. Appl. Sci. Res., 5 (2014) 139-147.

[15] G. Sreedevi, R. M. Vasudeva, P. Chinho, C. W. Jeon & R. K. T. Rama-krishna, Comprehensive Optical Studies on SnS Layers Synthesized by Chemical Bath Deposition, Opt. Mater., 42 (2015) 468–475. https://doi.org/10.1016/j.optmat.2015.01.043

[16] P.E .Agbo, P.A. Nwofe,Structural and optical properties of sulphurised Ag_2S thin films, Int. J. Thin Film Sci. Technol., 4 (2015) 9-12. http://dx.doi.org/10.12785/ijtfst/040102

[17] S. A. Gaikwad, Y. D. Tembhurkar , C. M. Dudhe, Effect of Substrate Temperature on Optical and Electrical Properties of CdZnSeTe Thin Films Prepared by Spray Py-rolysis Technique, Int. J. Dev. Res., 12 (2017) 17771-17775.

[18] Mursal, Ibrahim, Bukhari, & Z. Jalil, Structural and Optical Properties of Zinc Oxide (ZnO) based Thin Films Deposited by Sol-Gel Spin Coating Method , J. Phys.: Conf. Ser., 1116 (2018) 032020. https://doi.org/10.1088/1742-6596/1116/3/032020

[19] R. A. Busari, Tuning the optical properties and some surface structure of Cd-O thin film electrodeposited by two-electrode: An effect of Cobalt incorporation, J. Niger. Soc. Phys. Sci., 5 (2023) 1222. https://doi.org/10.46481/jnsps.2023.1222

[20] L. Fadillah, B. Soegijono and S. Budiawanti, Fabrication and characterization of ZnO and Li doped ZnO by a sol-gel method, AIP Conf. Proc., 1862 (2017) 030053. https://doi.org/10.1063/1.4991157

[21] V. A. Owoeye, E. Ajenifuja, E. A. Adeoye, G. A. Osinkolu & A. P. Popoola, Microstructural and optical proper-ties of Ni-doped ZnO thin films prepared by chemical spray pyrolysis technique, Mater. Res. Express., 6 (2019) 086455. https://doi.org/10.1088/2053-1591/ab26d9

[22] M. R. A. Bhuiyana & M. K. Rahmana, ,Synthesis and Characterization of Ni Doped ZnO Nanoparticles, Int. J. Eng. Manuf., 4 (2019) 10-17. https://doi.org/10.5815/ijem.2014.01.02

[23] R. V. Tolentino-Hernandez, E. Jimenez-Melero, F. J. Espinosa-Faller, C. Guarneros-Aguilar, & F. Caballero-Briones, One-step, low temperature synthesis of reduced gra-phene oxide decorated with ZnO nanocrystals using galva-nized iron steel scrap, Mater. Res. Express, 8 (2021) 065010. https://doi.org/10.1088/2053-1591/ac0c9c

[24] H. Ren, H. Weng, X. Dong, J. Huang & S. W. Joo, Nickel-Doped ZnO Porous Sea Urchin Nanostructures with Various Amounts of Oxygen Defects for Volatile Organic Compound, Chemosensors, 11 (2021) 223. https://doi.org/10.3390/chemosensors11040223

[25] L. Yang, Y. Zhao, R. Yin, & F. Li, Synthesis of Ni^{2+}-doped $ZnAl_2O_4$/ZnO Composite Phosphor Film with Largely Enhanced Polychromatic Emission via a Single-Source Precursor, J. Am. Ceram. Soc., 97 (2014) 1123–1130. https://doi.org/10.1111/jace.12748

[26] K. A. Mishjil, R. S. Abbas, Electronic transitions and optical properties of ZNO: in thin films, J. Multidiscip. Eng. Sci. Stud., 3 (2017) 1589-1598.

[27] K. A. Musiliyu, E. D. Ogunmola, A. A. Ajayi, et al.Effect of concentration on the properties of nitrogen-doped zinc oxide thin films grown by electrodeposition, Mater. Renew. Sustain. Energy, 12 (2023) 23–29. https://doi.org/10.1007/s40243-022-00225-0

[28] S. M. Ali, W. A. Farooq, M. R. Baig, M. A. Shar, M. Atif, S. S. Alghamdi, M S. Algarawi & M. H. Naeem-Ur-Rehman, Structural and optical properties of pure and Ag doped ZnO thin films obtained by sol gel spin coating tech-nique, Mater. Sci.-Pol.,, 33 (2015) 601-605. https://doi.org/10.1515/msp-2015-0091

[29] A. Bediaa, F. Z. Bediaa, M. Ailleriea, N. Maloufid, & B. Benyouce, Influence of the thickness on optical properties of sprayed ZnO hole-blocking layers dedicated to inverted organic solar cells, Energy Procedia, 50 (2014) 603–609. https://doi.org/10.1016/j.egypro.2014.06.074

[30] D. Taka, T. Onuma, T. Shibukawa, H. Nagai, T. Yamaguchi, J. S. Jang, M. Sato, & T. Honda, Fabrication of Ag dispersed ZnO films by molecular precursor method and application in GaInN blue LED, physica status solidi (a), 214 (2017) 1600598.

[31] J. I. Onwuemeka, & A. J. Ekpunobi, Synthesis of CdO:SnO_2 alloyed thin films for solar energy conversion and optoelectronic applications, J. Mater. Sci.: Mater. Electron., 29 (2018) 9176–9183. https://doi.org/10.1007/s10854-018-8945-z

[32] A. Hafdallah, F. Yanineb, M. S. Aida &N. Attaf, In doped ZnO thin films, J. Alloys Compd., 509 (2011) 7267–7270. https://doi.org/10.1016/j.jallcom.2011.04.058

[33] S. U. Offiah, P. E. Ugwoke, A. B. C. Ekwealor, S. C. Ezugwu, R. U. Osuji, & F. I. Ezema, Structural and Spec-tral Analysis of Chemical Bath Deposited Copper Sulfide Thin Films for Solar Energy Conversions, Dig. J. Nanomater. Biostruct., 7 (2012) 165–173.

[34] S. A. Moshgi, A. Afshar, & Y. Yaghoubinezhad, An Electrochemical Synthesis of Reduced Graphene Oxide/Zinc Nanocomposite Coating through Pulse-Potential Electrodepo-sition Technique and the Consequent Corrosion Resistance, Int. J. Corros., 2018 (2018) 1-13. https://doi.org/10.1155/2018/3028693